

PHYSICAL REVIEW B **81**, 134410 (2010)

Strain-induced half-metallic ferromagnetism in zinc blende CrP/MnP superlattice: First-principles study

Gul Rahman^{†*}*Department of Physics, University of Ulsan, Ulsan 680-749, Republic of Korea*

Abstract

Using first-principles calculations within generalized gradient approximation, the electronic and magnetic properties of zinc blende (zb) CrP/MnP superlattice are investigated. The equilibrium lattice constant is calculated to be 5.33 Å. The stability of ferromagnetic zb CrP/MnP superlattice against antiferromagnetism is considered and it is found that the ferromagnetic CrP/MnP superlattice is more stable than the antiferromagnetic one. It is shown that at the equilibrium lattice constant the CrP/MnP superlattice does not show any half metallicity mainly due to the minority t_{2g} states of Cr and Mn. However, if strain is imposed on the CrP/MnP superlattice then the minority t_{2g} electrons shift to higher energies and the proposed superlattice becomes a half-metal ferromagnet. The effect of tetragonal and orthorhombic distortions on the half metallicity of zb CrP/MnP superlattice is also discussed. It is also shown that InP-CrP/MnP/InP is a true half-metal ferromagnet. The half metallicity and magnetization of these superlattices are robust against tetragonal/ orthorhombic deformation.

PACS numbers: 71.20.-b, 75.50.Pp, 75.70.Cn

[†] Present Address: Graduate Institute of Ferrous Technology, Pohang University of Science and Technology, Pohang 790-784, Republic of Korea.

In the past decade, extensive research has been undertaken to explore the electron spin degree of freedom for the design of new electronic devices. This has been motivated by the prospect of using spin in addition, or as an alternative, to charge as the physical quantity carrying information, which may change device functionality to an entirely new paradigm: dubbed spintronics. One of the key requirements for engineering spintronics devices is the efficient injection of spin-polarized charge carriers from a terminal (that is, a ferromagnet electrode) into a semiconductor interlayer. A half-metal ferromagnet (HMF),¹ in which one spin channel is metallic while the other is semiconducting and hence 100% spin polarization at the Fermi level (E_F) is expected, is considered optimal for spintronic devices. After the discovery of HMF by Groot *et al.*¹ in 1983, much effort has been made to study new half-metallic compounds. Zinc blende (zb) transition metal pnictides and chalcogenides in their metastable state are among these new half-metallic compounds.^{2–8} Much attention was diverted to these zb compounds after the pioneering work of Akinaga *et al.*⁹ who predicted half-metallic behavior of zb CrAs grown as a thin film. The zb Cr(Mn) pnictides have been found to hold a large magnetic moment, i.e., 3.0 (4.0) μ_B for Cr (Mn) compounds, per formula unit.¹⁰ The calculated, using the full potential linearized augmented plane wave (FLAPW) method, equilibrium lattice constant of bulk zb CrP is found to be 5.35 Å and becomes a HMF for lattice constants ≥ 5.48 Å⁷ (a_{CP}). On the other hand the equilibrium lattice constant of zb MnP was calculated to be 5.308 Å, using the FLAPW, and was shown that zb MnP is not a HM at the equilibrium lattice constant.¹⁰ Note that, in nature, these zb type materials are stable in structures other than zb which do not show any half-metallic behavior.^{3,10–13} The previous theoretical calculations showed that the energy difference between zb and the natural structure, such as MnP and NiAs, are about 0.2–1.0 eV. However, it is argued that under epitaxial growth condition, most of the Cr and Mn pnictides and chalcogenides, the natural structure is either always lower in energy than zb or only becomes higher in energy under a lattice expansion that is larger than the ones that can be achieved by epitaxy on suitable semiconductor substrates.¹⁴ The ground state structure of MnP and CrP is orthorhombic (MnP-type)¹⁰ and attention is paid explicitly to zb type superlattices and to search for half metallicity in this superlattice.

In many cases, the spin polarization at E_F is sensitive to structural deformation and consequently the proposed HM often loses the high spin polarization in atomic disordered states at surface, interface, and other structures.¹⁵ The high degree of spin polarization at

the surface and interface is crucial for realistic applications. More recently, we calculated the magnetism of zb CrP (001) surface for different lattice constants and no surface states were found for the Cr-terminated surfaces, while the P-terminated surfaces destroyed the half-metallic behavior of zb CrP.¹⁶ The purpose of the present calculations is to search for a new HM layered material based on zb structure, i.e., CrP/MnP, and to see the effect of strain on electronic and magnetic properties. Here, it is shown that zb CrP/MnP superlattice does not show any half metallicity at its equilibrium lattice constant, but shows half-metallic behavior when external strain is applied.

The spin-polarized FLAPW method¹⁷ based on density functional theory in the generalized gradient approximation (GGA)¹⁸ was used for first-principles calculations. The core electrons were treated fully relativistically, whereas the valence electrons were treated semirelativistically. The basis functions were expanded in terms of spherical harmonics up to $l \leq 8$ inside each muffin-tin sphere and plane waves in the interstitial region, respectively. The muffin-tin radii were taken to be 2.20 a.u. for each atom in the calculations. Convergence with respect to the basis functions and k points was carefully checked. The layered structure of zb CrP/MnP considered in these calculations is shown in the inset of Fig. 1. The unit cell is tetragonal with lattice constant $c = \sqrt{a}$ and is highlighted with arrows. In the tetragonal primitive cell there are one Cr, one Mn, and two P atoms.

The equilibrium lattice constant of zb CrP/MnP layered structure is determined from the total energy calculations. To search for the equilibrium lattice constant, this parameter is varied from $\sim 5.0\text{\AA}$ to $\sim 6.0\text{\AA}$. A global energy minimum in the ferromagnetic (FM) state (see Fig. 1) with lattice constant of 5.33\AA (a_{eq}), which is close to the average of the equilibrium lattice constants of zb CrP and MnP, was found. To consider the stability of FM against the antiferromagnetic (AFM) configuration, a conventional unit cell (eight atoms unit cell) was used. It is also possible to use a tetragonal unit cell to consider only one type of AFM structure. However, two different types of AFM ordering, i.e., AFM coupling between Cr or Mn atoms (denoted as AFM1) and AFM coupling between Cr and Mn atoms (denoted as AFM2), were considered and a conventional unit cell was used. The FM state was found to be more stable than the AFM1 (AFM2) state by 0.71 (0.46) eV, which ensures that the true ground state of CrP/MnP superlattice is FM. The electronic structures were calculated for all lattice constants and very interestingly it was found that the CrP/MnP layered structure is a HMF for lattice constants $\geq 5.60\text{\AA}$ (a_{HM}), which will be discussed below.

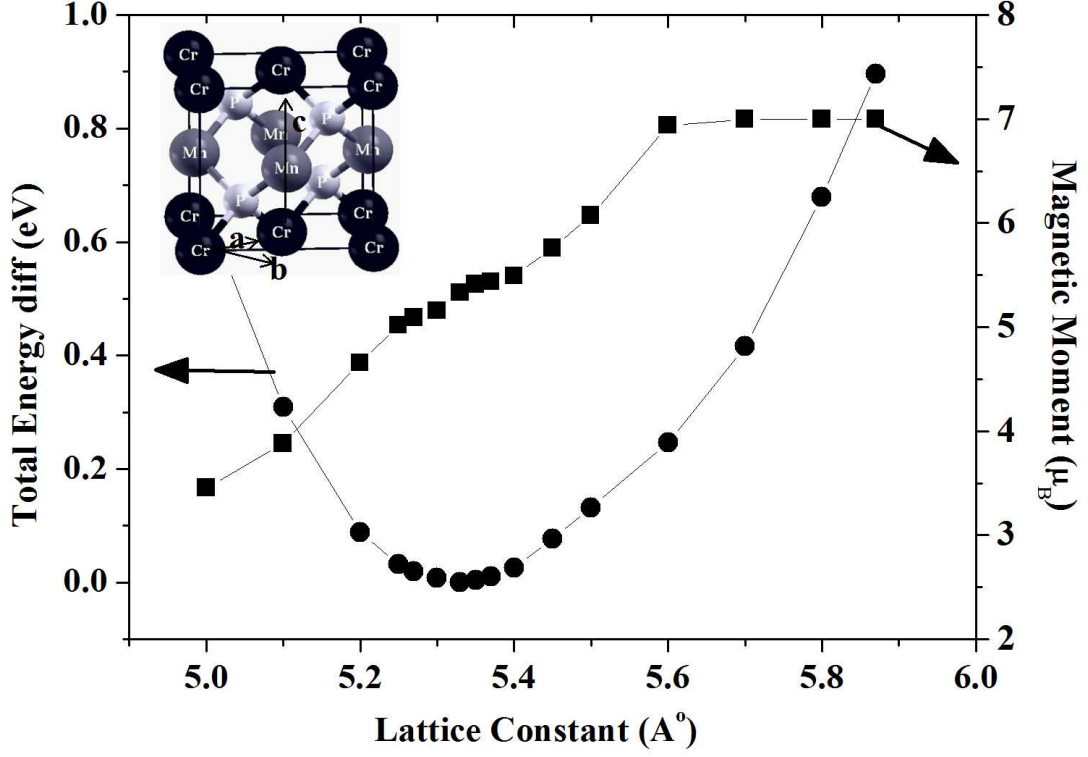


FIG. 1: The calculated total energy (eV) and magnetic moment (μ_B) vs lattice constant (\AA) of zb CrP/MnP superlattice. The filled circles (left panel) and squares (right panel) show the energies and magnetic moments. The inset on the top shows the conventional unit cell of the zb CrP/MnP superlattice and the arrows with labels a , b , and c represent the tetragonal unit cell. The total energy is given with respect to the equilibrium structure.

The calculated total and atom projected density of states (DOS) at a_{eq} are shown in Fig. 2(a). The Cr (Mn) d bands are decomposed into $t_{2g}(xy, yz, zx)$ and $e_g(x^2 - y^2, 3z^2 - r^2)$ states. The bands at ~ -10.0 eV (not shown) have anion s character and are well isolated from the bonding states so that they do not participate in bonding. The total DOS shows that the CrP/MnP superlattice is not a half-metal due to a finite DOS at E_F in the minority-spin states. The majority spin states in the interval -5.0 to -2.5 eV are bonding states and are formed by the Cr- and Mn- t_{2g} and P p electrons. The d nonbonding states, which are mainly formed by the e_g electrons of Cr and Mn, are located between ~ -2.5 eV and -1.2 eV. The antibonding states are around -1.0 eV and extend toward E_F . The minority spins

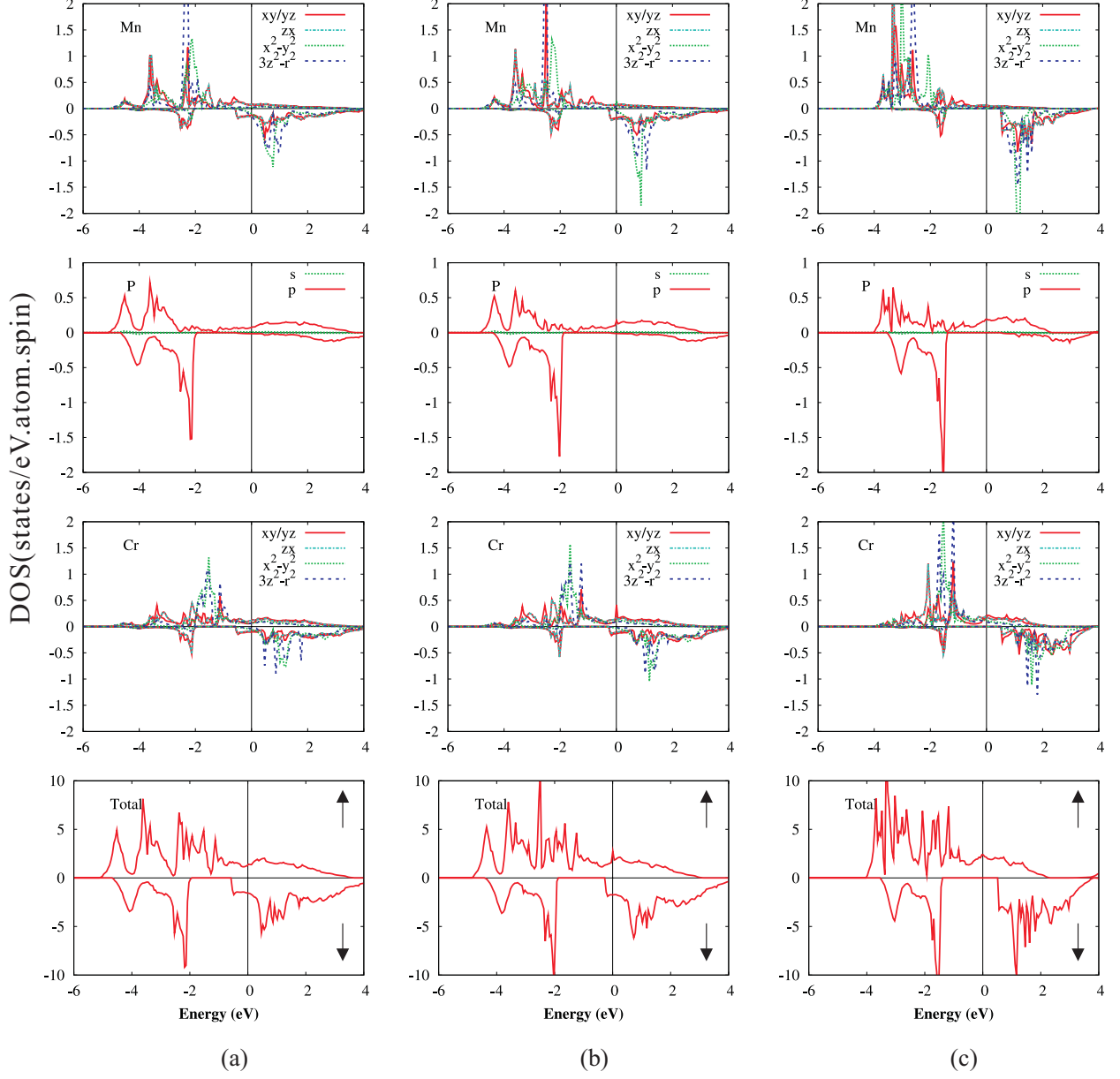


FIG. 2: The calculated total and atom projected densities of states of the zb CrP/MnP superlattice at (a) a_{eq} , (b) a_{CP} and (c) a_{HM} . The solid, dashed-dotted, dotted, and dashed lines show the xy/yz , zx , $x^2 - y^2$, and $3z^2 - r^2$ states, respectively. The thin solid and dotted lines represent the s and p states of P. The solid lines at the bottom panel show the total density of states. The up (down) arrows show the majority (minority) spins, and the Fermi level (E_F) is set to zero.

have hybrid bands between -5.0 eV and -2.0 eV, and the strong bonding peak ~ -2.0 eV is contributed by the t_{2g} electrons of Mn and Cr and the p electrons of P. The antibonding minority spins are located below E_F . The DOS at E_F is very large due to the minority spins which makes the CrP/MnP superlattice a metal. One can easily see that the CrP/MnP DOS is a mixture of Cr/Mn $3d$ states and the Mn states, which dominate the d manifold at lower energies. The Cr states dominate at higher energies, which is consistent with the nuclear charges. The t_{2g} states of Cr and Mn are responsible for the absence of half metallicity in the CrP/MnP superlattice. This happens because the exchange splitting between the bonding-antibonding is not strong at a_{eq} to push the minority spins to higher energies, which can open a band gap in the minority spin states. The DOS of zb CrP/MnP superlattice was also calculated at a_{CP} [see Fig. 2 (b)], which is larger than a_{eq} . It is noticeable that all the features of DOS of zb CrP/MnP superlattice at a_{CP} are similar to Fig. 2(a), i.e., absence of half metallicity. The DOS shows that with increasing the lattice constant, the minority conduction band moves to higher energy and E_F lies just above the conduction band minimum. This indicates the possibility of half metallicity in zb CrP/MnP superlattice.

The absence of half metallicity can be healed by volume expansion or by applying strain, which is not only used to control the carrier density, but also the mobility of the carriers.¹⁹ Strain is also considered to be a source to modify the electronic structure, magnetic and structural properties of materials.²⁰ As the lattice volume was increased (applying volumetric strain), it was found that the CrP/MnP superlattice developed insulating features in the minority spin states and the magnetic moment was also increased.

The calculated atom projected and the total DOS at a_{HM} are shown in Fig. 2(c). The DOS clearly shows that the CrP/MnP superlattice is a HM and now there are no minority states at E_F . For the majority band, the hybridization between the Mn t_{2g} and P p dominates between ~ -4.0 and -2.0 eV whereas above -2.0 eV, the Cr t_{2g} and P p bands are strongly hybridized. For the majority spins the conduction in the majority states is mainly dominated by the Cr d states. The minority spins exhibit a similar structure and the strong narrow bonding peak at ~ -1.80 eV is mainly contributed by the Cr t_{2g} and P p . The minority d states are shifted significantly relative to the majority d states by the exchange splitting and the d bands move to antibonding states, which open a gap (≥ 1.0 eV) that is important for spintronics. The states, which were formed between ~ -5.0 and -4.0 at a_{eq} , are shifted to higher energies due to strain. It is to be noted the t_{2g} states are completely occupied

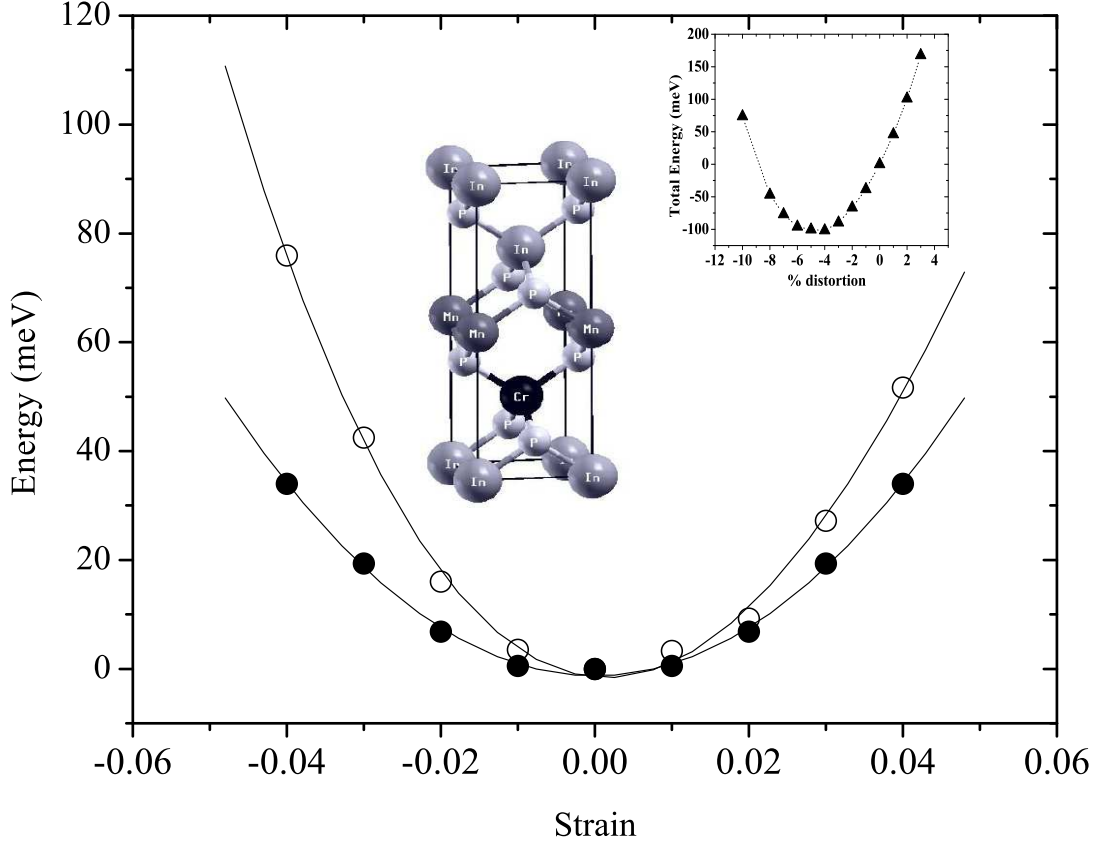


FIG. 3: Energy (meV) versus volume conserved tetragonal (open circles) and orthorhombic (filled circles) strains of zb CrP/MnP superlattice. The inset on the right top shows the total energy (meV) vs tetragonal distortion (%). The structure of InP-CrP/MnP/InP is also shown in the inset. The total energy is shown with respect to undistorted superlattices.

and the e_g states are empty. Comparing the effect of strain on CrP/MnP superlattice [Fig. 2(a) and (b)], one can see that the Cr/Mn $3d$ majority bands are narrowed by ~ 1.0 eV and the exchange splitting is increased for the Mn d bands. This large exchange splitting is accompanied by a large magnetic moment of the CrP/MnP superlattice (Fig. 1). Nevertheless, atomic disorder/antisite defects may affect the half metallicity.²¹

To further emphasis on the half-metallic behavior of zb CrP/MnP at a_{HM} , calculations were carried out on the effect of tetragonal and orthorhombic deformations on half metal-

licity. Volume conserved (Poisson's ratio= 0.5) distortions ($\pm 4\%$) were applied (see Fig. 3). It is clear to see that the half metallicity of zb CrP/MnP superlattice is robust to such distortions and the magnetic moment per cell remained constant. Similar behavior was also observed in other metastable zb CrAs and CrSb materials²² which have been grown successfully.^{9,23}

From the total energy and DOS calculations, it is concluded that it is necessary to apply strain for a transition FM metal to become a FM half-metal. The proposed strain may be produced if the CrP/MnP superlattice is grown on a substrate with lattice constant $> a_{\text{eq}}$. The strain will be generated by the lattice mismatch between a_{eq} and the substrate that will weaken the hybridization between the atoms. An example of material that can be used for this purpose is InP, whose experimental lattice constant of 5.87 \AA (a_{InP}) is larger than a_{eq} of the CrP/MnP superlattice. If CrP/MnP is grown on the InP substrate, which will induce some hydrostatic strain, then it is expected that the CrP/MnP will become a HMF.

It would be interesting to investigate the half metallicity of multilayer system, i.e., InP/MnP/CrP/InP, which can also be denoted as $\text{In}_{0.5}\text{Cr}_{0.5}\text{P} / \text{MnP} / \text{InP}$ or InP-CrP/MnP/ InP following the notation of Qian *et al.*²⁴ Further calculations were carried out for InP-CrP/MnP/InP superlattice (inset of Fig. 3) and it was found that this superlattice is also a HMF. The DOS of InP-CrP/MnP/InP system is shown in Fig. 4. The main features (half metallicity) are identical to the DOS at a_{HM} except a small band between -6.0 and -4.0 eV, which is mainly contributed by In atoms. More importantly, this system also has a band gap (~ 1.0 eV) in the minority spin states, but it is decreased compared with Fig. 2(c).

It is shown that the CrP/MnP superlattice can be a HMF even if it forms multilayer structure. Further, the effect of volume conserved tetragonal and orthorhombic distortions on half metallicity was also considered. It was found that the half metallicity is not affected by such distortions, similar to zb CrP/MnP superlattice. Then the stability of the half-metallic state of InP-CrP/MnP/InP against tetragonal distortion(tensile strain), which can be expected in real applications, is examined. A tetragonal distortion $\pm \%$ in the c direction was applied while keeping the in-plane lattice constant to find the energy minimum and see the effect of tensile strain on the magnetic moment and half metallicity. The calculated energy curve is shown in the inset of Fig. 3. The tetragonally distorted InP-CrP/MnP/InP has an energy minimum at about 4.5% compression. The corresponding energy change is ~ 0.10 eV with respect to the undistorted case. There are some reports where lattice mismatched($\sim 5\%$

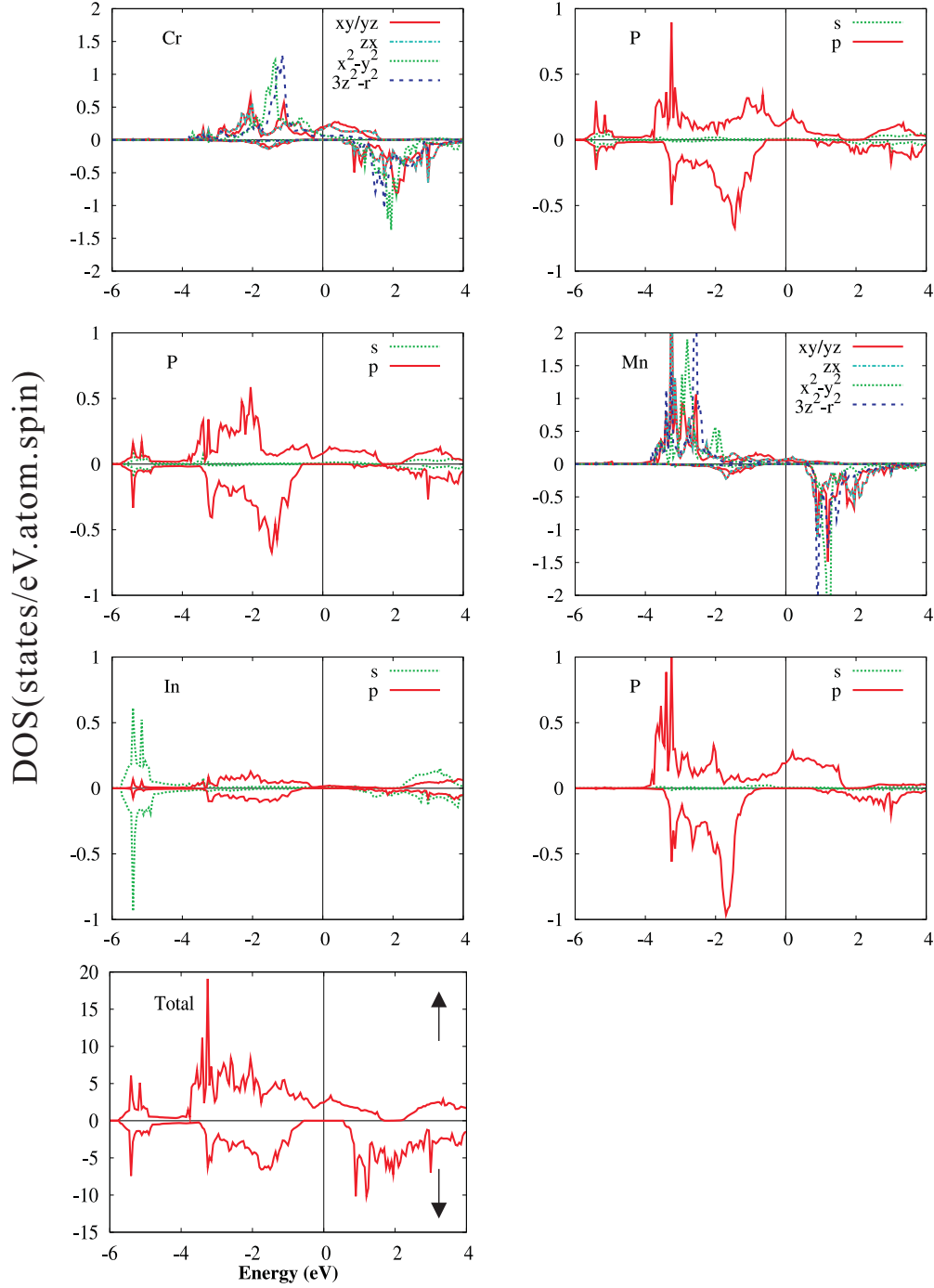


FIG. 4: The calculated total and atom projected density of states of InP-CrP/MnP/InP at a_{InP} . The solid, dashed-dotted, dotted, and dashed lines show the xy/yz , zx , $x^2 - y^2$, and $3z^2 - r^2$ states, respectively. The thin solid and dotted lines represent the s and p states of P. The solid lines at the bottom panel show the total density of states. The up (down) arrow shows majority (minority) spins and the Fermi level (E_F) is set to zero.

) superlattices are achieved successfully.^{25–28} More interestingly, the magnetic moment and the half-metallic behavior of InP-CrP/MnP/InP was not much affected by compression and elongation. When a zb half-metallic compound is grown on a semiconductor substrate [on (001)], its lattice will be tetragonally distorted so that it can assume the in-plane lattice constant of the semiconductor while approximately keeping its own atomic volume. Therefore, during the tensile strain the in-plane bond length between Cr or Mn and P atoms is the same as that of a_{InP} . The magnetic moments are already saturated at a_{InP} and the materials show half-metallic property (Fig. 1). The magnetic moment remains constant ($7.0\mu_B$) and the DOS for each case shows that the minority spin has a non-zero gap. The tetragonal distortion can have a strong effect on the half-metallicity if E_F lies at the edge of the gap. For InP-CrP/MnP/InP, E_F does not lie at the edge and then the half metallicity is not much affected. It is to be noted that if the distortion is too large, the half metallicity can be destroyed. These findings are encouraging because the interaction of CrP/MnP superlattice with InP will not cause loss of the half-metallic behavior. Furthermore, no interface states between CrP/MnP and InP were observed.

Finally, the total magnetic moment per unit cell for the CrP/MnP is also calculated and it is observed that the magnetic moment increases with the lattice constant, as shown in Fig. 1. The increase in the magnetic moment with the lattice constant is due to the increase in bond length (weak hybridization coming from a reduced p - d coupling) and is also observed in other zb materials.¹¹ The magnetic moment becomes saturated beyond 5.60 \AA and presents an integer value of $7.0\mu_B$, which is the sum of the free magnetic moments of Cr($3.0\mu_B$) and Mn($4.0\mu_B$).

The proposed material is a HMF at a_{HM} and shares a common minority electronic structure with the constituent compounds, i.e., zb CrP and zb MnP, where p - t_{2g} hybrid orbital are filled and e_g states are empty. The magnetic moment per formula unit (M) of the half-metallic zb transition metal pnictides superlattice is given by²⁹

$$M = (Z_t - 8N_P) \quad (1)$$

where Z_t is the total number of valence electrons in the unit cell and N_P is the number of P atoms per unit cell. For the CrP/MnP superlattice, $Z_t = 23$ and $N_P = 2$ and hence Eq.1 predicts a total magnetic moment of $7.0\mu_B$ per unit cell, which is confirmed by first-

principles all-electron FLAPW calculations.

In summary, first-principles calculations, using the FLAPW method within the GGA for the exchange and correlation potential, were performed to investigate the magnetic and electronic structures of zb CrP/MnP superlattices. The equilibrium lattice constant (5.33 Å) was determined from the total energy calculations. The stability of ferromagnetism against antiferromagnetism was also considered and it was shown that the ferromagnetic zb CrP/MnP superlattice is more stable than the antiferromagnetic superlattice. The electronic structures revealed that the zb CrP/MnP superlattice is not a true half-metal and the absence of half metallicity was discussed in terms of exchange splitting of the d states of Cr and Mn. However, the zb CrP/MnP superlattice became half-metal when strain was imposed. The half metallicity of strained CrP/MnP superlattice was not destroyed by tetragonal and orthorhombic deformations. The magnetization and half-metallic behavior of zb InP-CrP/MnP/InP was also discussed and it was found that the magnetic and electronic properties of this superlattice are not much affected by tetragonal distortion.

The author thanks Soon Cheol Hong and In Gee Kim for useful discussions. This work was partially supported by the Steel Innovation Program by POSCO through POSTECH and the Basic Science Research Program (Grant No. 2009-0088216) through the National Research Foundation funded by Ministry of Education, Science and Technology of Republic of Korea.

* Electronic address: grnphysics@yahoo.com

- ¹ R. A. de Groot , F. M. Mueller, P. G. van Engen, and K. H. J. Buschow, Phys. Rev. Lett. **50**, 2024 (1983).
- ² B. Sanyal, L. Bergqvist and O. Eriksson, Phys. Rev. B. **68**, 054417 (2003).
- ³ Y.-Q. Xu, B.-G. Liu, and D. G. Pettifor, Phys. Rev. B **66**, 184435 (2002).
- ⁴ J.-C. Zheng and J. W. Davenport, Phys. Rev. B. **69**, 144415 (2004).
- ⁵ M. S. Miao and W. R. L. Lambrecht, Phys. Rev. B. **72**, 064409 (2005).
- ⁶ W.-H. Xie, Ya-Q. Xu, B.G. Liu, and D. G. Pettifor, Phys. Rev. Lett. **91**, 037204 (2003).
- ⁷ J. E. Pask, L. H. Yang, C. Y. Fong, W. E. Pickett, and S. Dag, Phys. Rev. B **67**, 224420 (2003).
- ⁸ M. S. Miao and W. R. L. Lambrecht, Phys. Rev. B **71**, 064407(2005).
- ⁹ H. Akinaga, T. Manago and M. Shirai Jpn. J. Appl. Phys., Part 2 **39**, L1118 (2000).
- ¹⁰ A. Continenza, S. Picozzi, W. T. Geng, and A. J. Freeman, Phys. Rev. B **64**, 085204 (2001).
- ¹¹ S. Sanvito and N. A. Hill, Phys. Rev. B. **62**, 15553 (2000).
- ¹² J. I. Lee and S. C. Hong, J. Appl. Phys. **101**, 09G502 (2007).
- ¹³ P. Ravindran, A. Delin, P. James, B. P. Johansson, J. M. Wills, R. Ahuja, and O. Eriksson, Phys. Rev. B. **59**, 15680 (1999).
- ¹⁴ Y.-J. Zhao and A. Zunger, Phys. Rev. B **71**, 132403 (2005).
- ¹⁵ G. A. de Wijs and R. A. de Groot, Phys. Rev. B **64**, 020402(R) (2001).
- ¹⁶ G. Rahman, S. Cho, and S. C. Hong, J. Magn. Magn. Mater. **304**, e146 (2006).
- ¹⁷ E. Wimmer, H. Krakauer, M. Weinert, and A. J. Freeman, Phys. Rev. B **24**, 864 (1981).
- ¹⁸ J. P. Perdew, K. Burke, and M. Ernzerhof, Phys. Rev. Lett. **77**, 3865 (1996).
- ¹⁹ C.-G Duan, R. F. Sabiryanov, J. Liu, and W. N. Mei, P. A. Dowben, and J. R. Hardy, Phys. Rev. Lett. **94**, 237201 (2005).
- ²⁰ L. M. Falicov, D. T. Pierce, S. D. Bader, R. Gronsby, K. B. Hathaway, H. J. Hopster, D. N. Schuller, and R. H. Victora, J. Mater. Res. **5**, 1299 (1990).
- ²¹ I. Galanakis and S. G. Pouliazis, J. Magn. Magn. Mater. **321**, 1084 (2009).
- ²² L.-J. Shi and B.-G. Liu, J. Phys.: Condens. Matter. **17**, 1209 (2005).
- ²³ J. H. Zhao, F. Matsukura, K. Takamura, E. Abe, D. Chiba, and H. Ohno, Appl. Phys. Lett. **79**, 2776 (2001).

- ²⁴ M. C. Qian, C. Y. Fong, W. E. Pickett, J. E. Pask, L. H. Yang, and S. Dag, Phys. Rev. B **71**, 012414 (2005).
- ²⁵ R. L. Gunshor, L. A. Kolodziejewski, O. Ostuka, B. P. Gu, D. Lee, Y. Hafetz, and A. V. Nurmikko, Superlattices Microstruct. **3**, 5 (1987).
- ²⁶ H. Fujiyasu, Y. Takeuchi, K. Hikida, T. Kichi, K. Masuo, Y. Gotou, K. Ishino, and A. Ishida, J. Electron Mater. **22**, 545 (1993).
- ²⁷ M. Willatzen, L. C. Lew Yan Voon, P. V. Santos, M. Cardona, D. Munzar, and N. E. Christensen, Phys. Rev. B **52**, 5070 (1995).
- ²⁸ U. Schmid, N. E. Christensen, M. Alouani, and M. Cardona, Phys. Rev. B **43**, 14597 (1991).
- ²⁹ C. Y. Fong, M. C. Qian, J. E. Pask, L. H. Yang, and S. Dag, Appl. Phys. Lett. **84**, 239 (2004).